Journal of Magnetic Resonance 208 (2011) 291–297

Contents lists available at ScienceDirect

Journal of Magnetic Resonance

journal homepage: www.elsevier.com/locate/jmr

Communication

A radiofrequency coil configuration for imaging the human vertebral column at 7 T

M. Vossen [a], W. Teeuwisse [a,b], M. Reijnierse [a], C.M. Collins [c], N.B. Smith [a,b], A.G. Webb [a,b,*]

[a] Department of Radiology, Leiden University Medical Center, The Netherlands
[b] C.J. Gorter Center for High Field Magnetic Resonance Imaging, Leiden, ZA 2333, The Netherlands
[c] Center for NMR Research, Hershey Medical School, Hershey, PA, USA

ARTICLE INFO

Article history:
Received 12 May 2010
Revised 9 November 2010
Available online 4 December 2010

Keywords:
High-field RF coils
Spinal imaging
Phased arrays

ABSTRACT

We describe the design and testing of a quadrature transmit, eight-channel receive array RF coil configuration for the acquisition of images of the entire human spinal column at 7 T. Imaging parameters were selected to enable data acquisition in a clinically relevant scan time. Large field-of-view (FOV) scanning enabled sagittal imaging of the spine in two or three-stations, depending upon the height of the volunteer, with a total scan time of between 10 and 15 min. A total of 10 volunteers have been scanned, with results presented for the three subjects spanning the range of heights and weights, namely one female (1.6 m, 50 kg), one average male (1.8 m, 70 kg), and one large male (1.9 m, 100 kg).

1. Introduction

MRI is the preferred clinical imaging modality for musculoskeletal (MSK) applications due to the high soft tissue contrast, direct visualization of anatomic structures in multiple planes, and lack of ionizing radiation [1]. Standard clinical MSK imaging of the human vertebral column is performed using T_1, T_2 and/or proton density (PD) weighted fast spin echo and gradient echo sequences, with in-plane resolutions of ~1 mm and slice thickness of ~3–5 mm. Increasing the field strength from 1.5 to 3 T has already shown several advantages in human spinal imaging [2]. An approximately twofold increase in signal-to-noise ratio (SNR) improves image quality in terms of increased spatial resolution, faster image acquisition, and higher contrast in sequences such as diffusion weighting which are inherently SNR limited, and also improved contrast due to mechanisms such as magnetic susceptibility that are highly field strength dependent [2]. With the relatively recent advent of commercial 7 T scanners, MSK imaging using 7 T MRI is a research area of growing interest [3–12]. Given the results of 3 T MSK imaging, MRI at 7 T may have additional value in terms of higher spatial resolution and different types of contrast, to enhance visualization of morphologic changes [3].

Imaging of the human vertebral column at high-field is one of MSK's most challenging applications. The location of the human spine close to the center of the body makes high demands on radiofrequency (RF) coil design, and can lead to very low SNR in the anterior part of the spine. In order to image the entire spinal cord in two or three positions of the patient table, a large field-of-view (FOV) must be acquired while maintaining high spatial resolution. Currently no commercial 7 T system offers either a body transmit coil or dedicated RF receive coils for the spine. In designing appropriate RF coils, one has to contend with the well-characterized increase in magnetic field (B_1) inhomogeneities caused by the high dielectric constant of tissue, the decreased electromagnetic wavelength in tissue at high-fields, and also the increased specific absorption rate (SAR) [13–16]. Although not specifically targeting the spinal cord, Vaughan et al. [16] have shown, using a highly sophisticated whole-body transmit/receive TEM resonator, that images of the spinal cord can be acquired at 7 T. Other groups have designed coils at 7 T to study specific sections of the vertebral column. Wu et al. [8] used a transceiver array consisting of eight non-overlapping microstrip loop elements, with novel adjustable inductive decoupling networks between each element of the array. The length of the array was ~50 cm, which was shown to be sufficient to be able to cover the lumbar spine. Parallel imaging with a reduction factor of up-to-four was shown to be feasible using this RF coil setup. A particularly interesting design has been shown by Kraff et al. [17]. They used an eight element transmit/receive array consisting of two rows of shifted, overlapping square structures in which a 180° phase shift was introduced between the two rows of elements to increase the B_1^+ amplitude along the centerline of the coil, while simultaneously canceling out the signal from tissue either side of the centerline. Using this approach they were able to acquire three-dimensional gradient echo images with very high spatial resolution, and also show that parallel imaging techniques could successfully be implemented. Images of either the cervical or thoracic spine could be acquired over a 40 cm field-of-view using this coil arrangement. Excellent visualization of small structures, particularly in the posterior part of the vertebral column,

* Corresponding author. Address: C.J. Gorter Center for High Field MRI, Department of Radiology, C3-Q, Leiden University Medical Center, Albinusdreef 2, Leiden, 2333 ZA, The Netherlands. Fax: +31 71 524 8256.
E-mail address: a.webb@lumc.nl (A.G. Webb).

1090-7807/$ - see front matter © 2010 Elsevier Inc. All rights reserved.
doi:10.1016/j.jmr.2010.11.004

was achieved, accompanied with the expected signal drop-off towards the anterior side of the spine.

In this paper we present an alternative setup, which is specifically tailored towards clinical applications in diseases such as ankylosing spondylitis (AS) [18], in which it is important to have a reasonably homogeneous field on both anterior and posterior sides of the vertebral column, as well as to have a large coverage in the head/foot direction so that the entire spine can be imaged in two-stations for normal, or three-stations for very tall, subjects. For applications to spine imaging it is important to note that SAR is highly dependent upon the nature of the tissue through which the RF fields have to propagate. For example, the total power deposited in the body might be anticipated to be lower if the RF energy is transmitted through the lungs from the anterior side to the centrally located spinal cord, than if the RF coil were to be placed in exactly the same head/foot position on the posterior side of the body, in which case the RF field must propagate through a large muscle mass with high conductivity. A similar suggestion was initially made by Vaughan et al. [16]. Therefore, we based our transmit design on a simple quadrature RF coil setup which is placed on the anterior side of the patient. The receive coil is an eight-element overlapped design, with total length of ~90 cm, such that the entire spinal cord can be imaged without requiring the patient to move. For multi-station imaging, the quadrature transmit coil is simply repositioned and the patient table moved to the new position.

2. Methods

All imaging protocols were approved by the Leiden University Medical Center medical ethics committee. Ten healthy adult volunteers, both men and women, were studied on a commercial human whole-body 7 T MR system (Philips Achieva, Philips Healthcare, Best, The Netherlands). All subjects were positioned head first and in a supine position in the magnet. The RF amplifier delivers a maximum of 1 kW to each quadrature transmit channel, measured at the input to the RF coil.

2.1. Electromagnetic simulations

Electromagnetic simulations were performed using a discretized model of the human body [13] and a finite-difference time-domain (FDTD) method with commercially-available software (xFDTD, Remcom Inc, State College, PA, USA). The three-dimensional body model was segmented into 75 different tissue types, with appropriate conductivity and dielectric properties assigned to each tissue [13]. A mesh size of $5 \times 5 \times 5$ mm was used for all simulations. Computational time on an 8-core PC was approximately 20 min for SAR and rotating B_1^+ fields throughout the volume of interest.

2.2. RF coil construction

Since only two quadrature transmit channels are currently available on the commercial Philips 7 T system, multi-transmit array technology which has been used for previous high-field spine studies [8,16,17] could not be incorporated. Instead, the transmit coil is a quadrature double-loop design, with appropriate overlap between the two loops to minimize the mutual inductance [19]. The diameter of each loop is 20 cm with an overlap of ~3 cm. Each loop is segmented into eight separate sections with 3.9 pF non-magnetic capacitors (American Technical Ceramics, Series B, Huntington Station, NY) and one 1–30 pF variable capacitor (Johansson, Camarillo, CA) for fine tuning. Balanced impedance matching was achieved using one 1–40 pF variable and one fixed 33 pF capacitor. A 1-cm thick foam padding was placed between the coil and the subject. Each loop was impedance matched at 298.1 MHz with an S_{11} measurement of lower than −20 dB when the coil was placed on the subject. The isolation under loaded conditions between each channel was between −18 and −24 dB for each subject studied. The unloaded and loaded Q values were 150 and 20, respectively. A detuning voltage of +12 V is supplied from the spectrometer, and is used to drive a conventional active PIN-diode decoupling circuit [20].

The receive coil is an eight-element array, shown schematically in Fig. 1, with each element being octagonal in shape and split by five 3.9 pF fixed value series capacitors and one 1–30 pF variable capacitor for fine tuning. Balanced impedance matching, an LC lattice balun, and small "figure-8 cable traps" were placed in front of each element of the array. The more common cable-traps are loops of coaxial-cable wound to make an inductor with a capacitor across the gap in the shield to resonate the shield. This configuration produces an extra B-field which can either produce unwanted signal or interfere with the main coil if it is placed very close. By wrapping the coaxial-cable into a figure-eight rather than single loop, any extraneous B-field is reduced. Each element in the coil is ~14 cm wide in the z-dimension, and is overlapped by ~2 cm in this direction. The total length of the array is 91 cm. The coaxial-cables (length ~1 m) attached to each element of the array are grounded together at the coil, and again at a distance approximately one-quarter wavelength away. This significantly reduces the effects of the environment within the magnet interacting with the RF cables. A 1-cm thick piece of foam was placed on top of the RF coil, on which the subject lies. Each element was impedance matched to less than −20 dB on the S_{11} measurement, with nearest neighbor coil isolation greater than −15 dB, and next-nearest neighbour greater than −25 dB, when loaded. A detuning voltage of −3.6 V is supplied for each channel from the spectrometer, and is used to power two active PIN-diode decoupling circuits [20] across the variable tuning and matching capacitors. Additional passive cross-diode circuits are used for each coil. The eight-coil array was interfaced to the commercial Philips interface box which contains preamplifiers with an input impedance of 6-j5 Ohms.

A long thin plastic bag (95 cm length, 15 cm width, 7 mm thick), filled with 3:1 weight/weight calcium titanate in deionized water was placed directly on top of the RF coil array below the subject's spine. This material has a dielectric constant of ~110 and has been shown to increase the B_1 homogeneity at high-fields [21].

2.3. Data acquisition parameters

A variety of imaging protocols were explored in terms of sensitivity to motion artifacts, signal-to-noise efficiency per unit time, image contrast and SAR. The final sequence used is a multiple slice two-dimensional gradient echo sequence, acquired in the sagittal orientation (as are most clinical scans at lower field), without respiratory triggering: TR/TE 15/2 ms (partial echo acquisition), field-of-view 450×240 mm, data matrix 600×320, in-plane resolution 0.75×0.75 mm, 3 mm slice thickness, 0.3 mm interslice gap, eight signal averages, seven slices, total data acquisition time ~4 min. Eight signal averages were acquired primarily to limit motion artifacts from cardiac motion since the effective use of saturation bands causes a substantial SAR penalty. Since the coverage (left/right) through the spinal column might not be sufficient for some applications, we have also performed imaging with 14-slices, total coverage 6 cm, with four signal averages and the same total data acquisition time. Data acquisition parameters were chosen to remain within the International Electrotechnical Committee (IEC) guidelines on peak and time-averaged SAR. Due to SAR limitations, sequences that can currently be used are limited to gradient echoes. For imaging the cervical/upper thoracic spine,

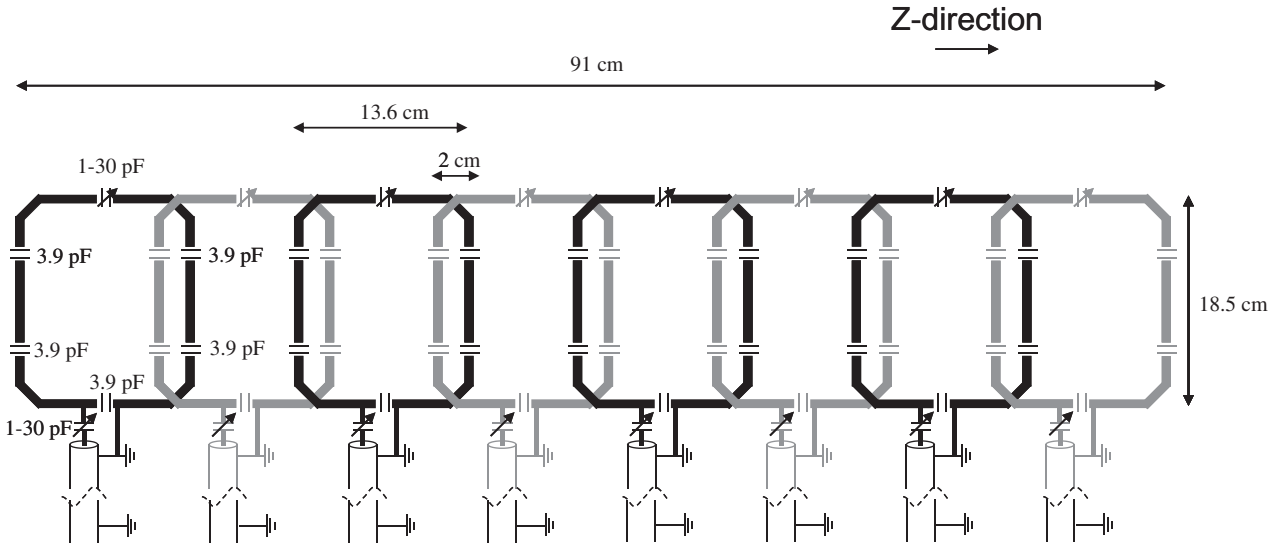

	1	2	3	4	5	6	7	8
1	1	0.1	0.02	0.003	0.009	0.01	0.01	0.02
2		1	0.09	0.09	0.01	0.02	0.01	0.01
3			1	0.07	0.02	0.03	0.01	0.01
4				1	0.09	0.18	0.06	0.02
5					1	0.15	0.04	0.03
6						1	0.1	0.1
7							1	0.04
8								1

Fig. 1. (top) Schematic drawing of the eight-element receive array with relevant dimensions and capacitor values. The eight-coils are grounded together as close to the coil as possible, and then again at a distance approximately one-quarter wavelength down the identical-length RG-58 coaxial-cables. (bottom) Measured noise correlation matrix for the eight-element array loaded with a volunteer.

the top six elements of the receive array are used, and for the lower thoracic/lumbar spine the bottom four elements. Images are stitched together by simple estimation of the appropriate overlap with no further image processing.

2.4. Signal-to-noise and noise correlation measurements

Signal-to-noise measurements were performed on the magnitude images, by the standard procedure of dividing the mean signal intensity within a defined region-of-interest by the standard deviation of the noise. For measurements within CSF, the vertebral disk and the inter-vertebral space, five different regions of interest were taken. Five different noise regions were selected, taking care to avoid any areas in which the noise is artificially reduced (due to the Philips software) or in which motion-induced artifacts are present.

A noise correlation matrix was measured as described in Roemer et al. [19] with a volunteer in place, and processed in MATLAB (The Mathworks, Natick, MA).

3. Results

For the electromagnetic simulations, the bore of the magnet is modeled as a conductive RF copper shield. Each RF coil is capacitively split to produce a resonant frequency at 298.1 MHz. As shown in Fig. 2, three different positions of the RF coil were modeled, corresponding to imaging the upper cervical, mid-thorassic, and lower lumbar spinal column. In shorter subjects, sufficient coverage could be obtained using only two positions, but three positions were included for completeness.

In the situation in which the quadrature coil is placed on the upper chest, the measured B_1^+ per square root of power for the anterior portion of the spinal column has a value of 86.5 nT per square root Watts, corresponding to a value of ~4 μT for the maximum power delivery of 2 kW. The value with the coil placed on the upper back is 62 nT per square root Watts. The maximum value of the 10 g average SAR for the upper back configuration (0.62 W/kg per W input power) was 30% greater than that on the front (0.47 W/kg per W input power). For the configuration in which the transmit coil is placed roughly posterior or anterior to the heart, the spinal column bends much closer to the back of the body, and the B_1^+ values now slightly favor having the RF coil on the back of the subject: the respective values being 30 and 36 nT per square root Watts for the two arrangements. In these cases the maximum 10 g average SAR is identical with a value of 0.57 W/kg per W input power), although one might note that equal energy depositions in the highly perfused heart tissue and much poorer perfused muscle will result in much lower temperature increases in the former case. In the final, most inferior positioning of the transmit coil, again there is a significant increase in the B_1^+ per root power at the anterior portion of the spinal column by placing the coil at the front, with values of 65 and 57 nT per square root Watts, respectively. The maximum 10 g SAR values are 36% less for the coil placed at

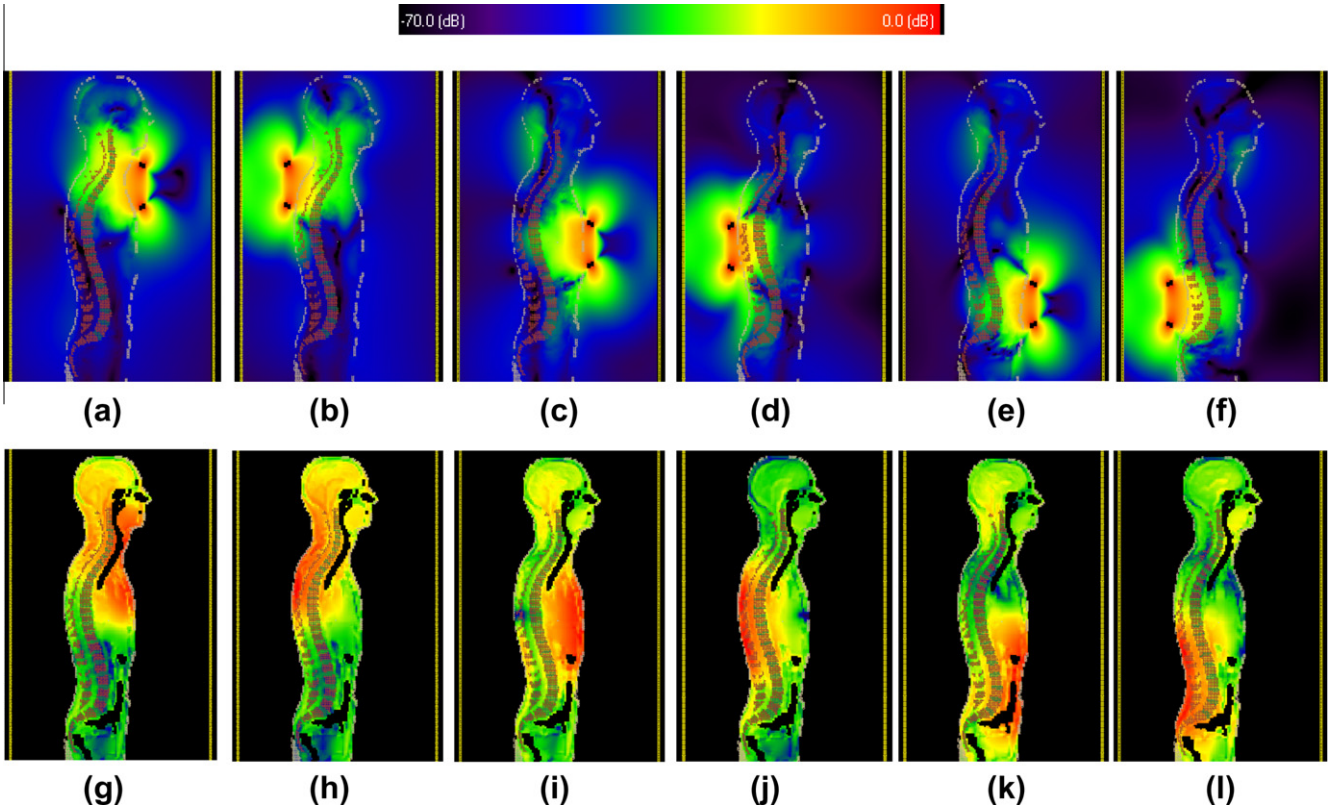

Fig. 2. Results from electromagnetic simulations of (top row) the rotating B_1^+ component of the transmit RF field, and (bottom row) the voxel-based SAR values. (a), (c), (e), (g), (i) and (k) show results with the quadrature transmit coil place anterior to the subject, with (b), (d), (f), (h), (j) and (l) with the coil placed in a posterior position. The values are plotted on a logarithmic scale. For the B_1^+ maps 0 dB corresponds to a value of 4.35 μT per square root Watts of input power, and for the SAR maps the corresponding value is 1.05 W/kg per Watt of input power.

the anterior side (0.41 W/kg per W input power) than that for the posterior arrangement (0.56 W/kg per W input power).

Fig. 3 shows images from the cervical spine of two different subjects, one male and one female. In terms of image appearance compared to 1.5 T scans, for example, the contrast is most similar to short time inversion recovery (STIR) images. In particular the contrast between the vertebral endplates and vertebral disks is very high, which could be beneficial in distinguishing endplate

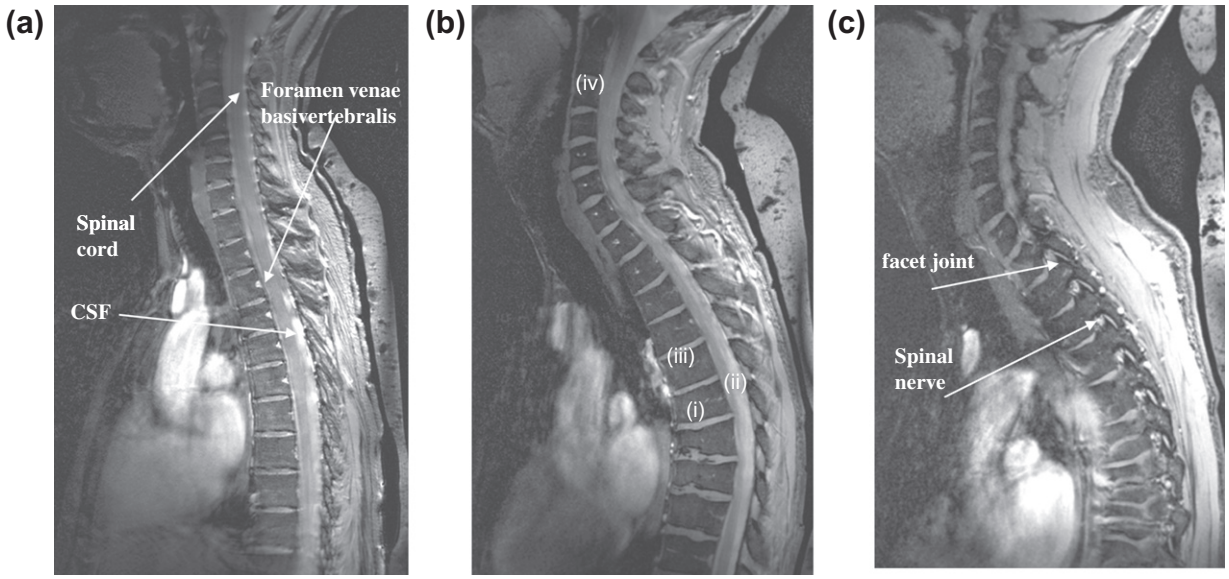

Fig. 3. Sagittal images through the cervical spine of a female (a), and male (b, c, two different slice positions) volunteers with the quadrature transmit coil positioned centrally on the chest with the upper edge placed against the chin. Despite the residual effects of cardiac motion fine structures such as the feeding vessels (foramen venae basivertebralis) can be discerned as areas of high intensity. There is good contrast between the CSF and the nerve fiber tracks and a relatively uniform signal intensity from the posterior and anterior sections of the vertebral column. Signal from the dielectric bag behind the back can be seen at the far right of the images. Female height/weight 1.7 m, 58 kg: male height/weight 1.8 m, 70 kg.

changes associated with diseases such as ankylosing spondylitis. As expected from gradient echo based sequences, there are no discernable flow effects, unlike would be seen on spin-echo images. Despite the very short T_2^* value (~2 ms) of the dielectric material [21], there is considerable signal due to the very short TE value used.

Signal-to-noise measurements were performed in the CSF, vertebral disk and inter-vertebral space, as indicated by positions (i), (ii), (iii) in the center of the field-of-view, and (iv) in the vertebral disk at the top of the cervical spine in Fig. 3b. The values were 15:1, 12:1, 2:1 and 10:1, respectively. These numbers were consistent with images in the upper thoracic spine images of other volunteers. The low value for the inter-vertebral space is expected due to the very low T_2^* value, and the fact that gradient echo rather than spin echo sequences were run. This contrast is very similar to that seen in previous studies at 7 T [8,16,17], although unfortunately previous authors do not report any signal-to-noise measurements which makes comparisons difficult.

One feature that can be seen in the central image of Fig. 3 was an unexpected collapsed vertebrae (authenticated later by a clinical scan on a 1.5 T system), characterized by the lack of intraosseous edema and therefore not a recent pathology. Fig. 4 shows expansions of this region, showing the very fine details in the collapsed vertebrae and inter-vertebral disks.

With a total length of 91 cm, the phased array coil can acquire data from the entire vertebral column. Fig. 5a and b shows images from the thoraco-lumbar spine of two other volunteers. Since an important question is how well the RF coil arrangement works with different patient sizes, a volunteer of >100 kg weight was chosen for the scan, shown in Fig. 5a. Signal-to-noise measurements for the CSF, vertebral column and inter-vertebral space (measured at the central position in the head/foot direction) were 17:1, 18:1 and 5:1, respectively. Fig. 5b shows results from a female volunteer, in which images were acquired at two positions of the patient bed, separated by ~25 cm. The quadrature transmit coil was shifted by the subject themselves from directly over the heart to immediately above the navel. The table was repositioned electronically and two sets of data collected immediately one after the other, and then "stitched together" as described previously. Fig. 6 shows results from the 14-slice, four signal average data set, with relatively little difference seen between this and the data sets with lower left/right coverage and higher signal averaging.

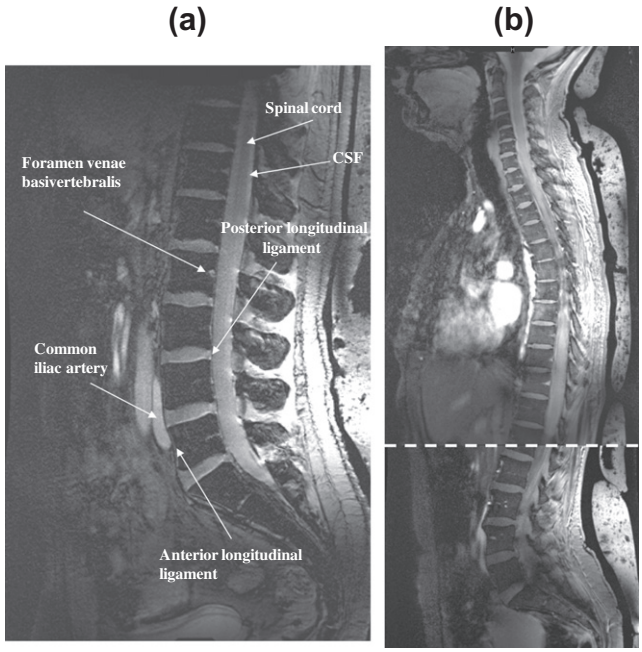

Fig. 5. (a) A mid-sagittal image of the lumbar spine acquired from a patient, height 1.9 m, who weighted over 100 kg. (b) Two mid-sagittal slices of a female volunteer (height 1.7 m, 50 kg weight) which are acquired at two different positions of the patient table and stitched together at the overlap point indicated by the dotted line. No intensity correction or image smoothing has been applied to either image.

Fig. 7 shows the effects of the high dielectric bag which is placed underneath the subject and directly on top of the RF coil. In

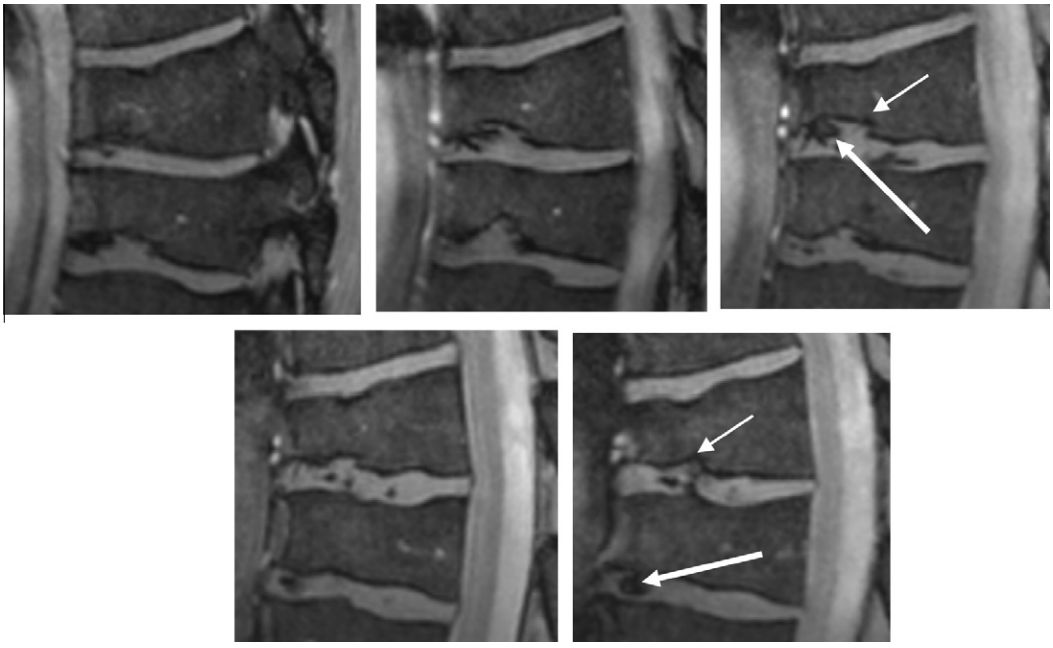

Fig. 4. Zoomed images of two collapsed vertebrae from Fig. 2b. Cortical irregularity of the endplates can be seen (thin arrows), consistent with osteochondrosis. The inter-vertebral disks show inhomogeneities (thick arrows) which could be based on califications in the disk or, alternatively, degeneration.

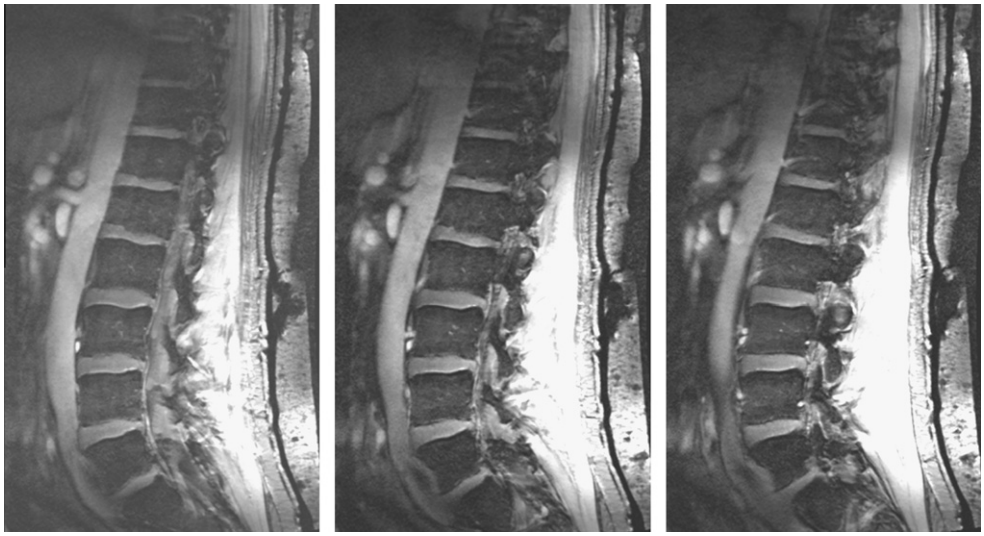

Fig. 6. Three adjacent sagittal slices from a 14-slice data set with improved left/right coverage of 6 cm, and a reduced number of signal averages (four), while maintaining the same total data acquisition time as for the other images.

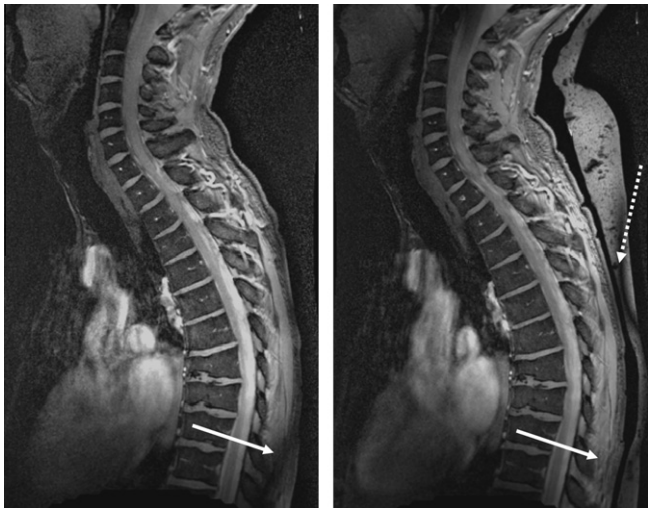

Fig. 7. Illustration of the effects of high dielectric material on the image quality. (left) Without bag and (right) with bag. Without the bag an area of low signal intensity caused by partial destructive interference of the RF field occurs within the patient as shown by the white arrow. With the addition of the bag, this effect is removed to a location within the dielectric material itself (dotted arrow).

particular the material is effective in "moving" the effects of signal cancelation from the body to the high dielectric material. The SNR within the vertebral column is identical with and without the bag.

4. Discussion

An RF coil arrangement is presented which enables imaging of the entire vertebral column at 7 T. Imaging parameters such as the spatial resolution have been matched to standard clinical scans enabling an imaging time of a few minutes. Based upon observations of the efficiency of RF transmission through the posterior and anterior sides of the body for previous cardiac studies [22], we adopted the approach of using a transmit coil placed on the anterior side of the patient to transmit through tissues with relatively low density (lungs, bowels) with resulting low RF attenuation and power deposition. Electromagnetic simulations suggest that this approach is advantageous for imaging the cervical spine and lumbar spine, with essentially identical results in the mid-thorassic region.

The use of a high dielectric material on the posterior side was found to minimize RF interference effects within the body. The most likely reason for this is that the RF energy has a much shorter wavelength in the dielectric than in air, and so the areas of low signal intensity typically found close to the overlapping areas of array receivers is moved outside of the body and into the dielectric itself. These effects occur at slightly different positions in different subjects. The shape, dimensions and material composition of the dielectric have not yet been optimized, and this is an area of current investigation. Although the material has very short T_2 and T_2^* values [21], it is clear that it does give very high signal on the images shown here which use a very short TE. An obvious solution to this is to construct the dielectric bags with deuterated rather than protonated water.

It can be anticipated that additional splitting of the transmit channels might well improve the image quality yet further, and the use of multiple transmit array elements is another obvious improvement that awaits hardware upgrades of the commercial systems. Nevertheless, perfectly useable images of the vertebral column can be acquired using the current RF setup, and issues of whether added clinical value can be provided by high-field imaging can begin to be addressed.

Acknowledgment

This work was funded by a grant from the AS Rheumafonds, "High sensitive imaging methods to assess relation between inflammation and syndesmophyte formation in Ankylosing Spondylitis".

References

[1] M.D. Shapiro, MR imaging of the spine at 3T, Magn. Reson. Imaging Clin. North Am. 14 (2006) 97–108.
[2] T.J. Mosher, Musculoskeletal imaging at 3T: current techniques and future applications, Magn. Reson. Imaging Clin. North Am. 14 (2006) 63–76.
[3] S. Banerjee, R. Krug, J. Carballido-Gamio, D.A. Kelley, D. Xu, D.B. Vigneron, S. Majumdar, Rapid in vivo musculoskeletal MR with parallel imaging at 7T, Magn. Reson. Med. 59 (2008) 655–660.
[4] R. Krug, C. Stehling, D.A.C. Kelley, S. Majumdar, T.M. Link, Imaging of the musculoskeletal system in vivo using ultra-high field magnetic resonance at 7 T, Invest. Radiol. 44 (2009) 613–618.
[5] R. Krug, J. Carballido-Gamio, S. Banerjee, A.J. Burghardt, T.M. Link, S. Majumdar, In vivo ultra-high-field magnetic resonance imaging of trabecular bone microarchitecture at 7 T, J. Magn. Reson. Imaging 27 (2008) 854–859.

[6] R. Krug, J. Carballido-Gamio, S. Banerjee, R. Stahl, L. Carvajal, D. Xu, D. Vigneron, D.A. Kelley, T.M. Link, S. Majumdar, In vivo bone and cartilage MRI using fully-balanced steady-state free-precession at 7 T, Magn. Reson. Med. 58 (2007) 1294–1298.
[7] R. Stahl, R. Krug, D.A. Kelley, J. Zuo, C.B. Ma, S. Majumdar, T.M. Link, Assessment of cartilage-dedicated sequences at ultra-high-field MRI: comparison of imaging performance and diagnostic confidence between 3.0 and 7.0 T with respect to osteoarthritis-induced changes at the knee joint, Skeletal Radiol. 38 (2009) 771–783.
[8] B. Wu, C.S. Wang, R. Krug, D.A. Kelley, D. Xu, Y. Pang, S. Banerjee, D.B. Vigneron, S.J. Nelson, S. Majumdar, X.L. Zhang, 7T Human spine imaging arrays with adjustable inductive decoupling, IEEE Trans. Biomed. Eng. 57 (2010) 397–403.
[9] G. Chang, K.M. Friedrich, L. Wang, R.L. Vieira, M.E. Schweitzer, M.P. Recht, G.C. Wiggins, R.R. Regatte, MRI of the wrist at 7 tesla using an eight-channel array coil combined with parallel imaging: preliminary results, J. Magn. Reson. Imaging 31 (2010) 740–746.
[10] G. Chang, S.K. Pakin, M.E. Schweitzer, P.K. Saha, R.R. Regatte, Adaptations in trabecular bone microarchitecture in Olympic athletes determined by 7T MRI, J. Magn. Reson. Imaging 27 (2008) 1089–1095.
[11] K.M. Friedrich, G. Chang, R.L. Vieira, L. Wang, G.C. Wiggins, M.E. Schweitzer, R.R. Regatte, In vivo 7.0-tesla magnetic resonance imaging of the wrist and hand: technical aspects and applications, Semin. Musculoskelet. Radiol. 13 (2009) 74–84.
[12] L. Wang, Y. Wu, G. Chang, N. Oesingmann, M.E. Schweitzer, A. Jerschow, R.R. Regatte, Rapid isotropic 3D-sodium MRI of the knee joint in vivo at 7T, J. Magn. Reson. Imaging 30 (2009) 606–614.
[13] C.M. Collins, M.B. Smith, Calculations of B1 distribution, SNR, and SAR for a surface coil adjacent to an anatomically-accurate human body model, Magn. Reson. Med. 45 (2001) 692–699.
[14] C.M. Collins, Q.X. Yang, J.H. Wang, X. Zhang, H. Liu, S. Michaeli, X.H. Zhu, G. Adriany, J.T. Vaughan, P. Anderson, H. Merkle, K. Ugurbil, M.B. Smith, W. Chen, Different excitation and reception distributions with a single-loop transmit-receive surface coil near a head-sized spherical phantom at 300 MHz, Magn. Reson. Med. 47 (2002) 1026–1028.
[15] C.M. Collins, W. Liu, W. Schreiber, Q.X. Yang, M.B. Smith, Central brightening due to constructive interference with, without, and despite dielectric resonance, J. Magn. Reson. Imaging 21 (2005) 192–196.
[16] J.T. Vaughan, C.J. Snyder, L.J. DelaBarre, P.J. Bolan, J. Tian, L. Bolinger, G. Adriany, P. Andersen, J. Strupp, K. Ugurbil, Whole-body imaging at 7T: preliminary results, Magn. Reson. Med. 61 (2009) 244–248.
[17] O. Kraff, A.K. Bitz, S. Kruszona, S. Orzada, L.C. Schaefer, J.M. Theysohn, S. Maderwald, M.E. Ladd, H.H. Quick, An eight-channel phased array RF coil for spine MR imaging at 7 T, Invest. Radiol. 44 (2009) 734–740.
[18] J. Sieper, M. Rudwaleit, X. Baraliakos, J. Brandt, J. Braun, R. Burgos-Vargas, M. Dougados, K.G. Hermann, R. Landewe, W. Maksymowych, H.D. van der, The Assessment of spondylarthritis international society (ASAS) handbook: a guide to assess spondylarthritis, Ann. Rheum. Dis. 68 (Suppl. 2) (2009) ii1–44.
[19] P.B. Roemer, W.A. Edelstein, C.E. Hayes, S.P. Souza, O.M. Mueller, The NMR phased array, Magn. Reson. Med. 16 (1990) 192–225.
[20] W.A. Edelstein, C.J. Hardy, O.M. Mueller, Electronic decoupling of surface-coil receivers for NMR imaging and spectroscopy, J. Magn. Reson. 67 (1986) 156–161.
[21] K. Haines, N.B. Smith, A.G. Webb, New high dielectric constant materials for tailoring the B1+ distribution at high magnetic fields, J. Magn. Reson. 203 (2010) 323–327.
[22] S.G. van Elderen, M.J. Versluis, A.G. Webb, J.J. Westenberg, J. Doornbos, N.B. Smith, R.A. de, M. Stuber, Initial results on in vivo human coronary MR angiography at 7 T, Magn. Reson. Med. 62 (2009) 1379–1384.